



Article submitted to journal

Subject Areas:

Climate Sensitivity

Keywords:

Regional Climate Sensitivity, Impulse Response, ARX method, Ljung-Box test

Author for correspondence:

J. S. Reid

e-mail: johnsinclairreid@gmail.com

Estimating Climate Sensitivity

J. S. Reid¹ and P. J. Nielsen²

¹33 Charlotte Street, New Norfolk, Tas., Australia. 7140

²12 View Street, Sandy Bay, Tas., Australia. 7005

We use a statistical method to estimate both global and regional climate sensitivity from observed time series while making no assumptions about the underlying physics.

1. Introduction

Thirty years ago one of us presented a paper to a symposium on wave breaking[1] at which many leading researchers in the field were present. It described a simple experiment in a wave tank which clearly demonstrated that frequency downshifting in surface gravity waves is caused by white-capping. The paper was greeted with outrage by many of those present, one of whom was given the floor for an immediate rebuttal with the argument that, if the proposal were true, many years of good work on wave models would have been wasted. In the field of gravity wave dynamics, theory reigned supreme and meticulous experiment and observation were anathema.

Science has no parallel discipline similar to historiography and so there is little examination of underlying assumptions and prejudices. The seminal works of Popper[2] and of Kuhn[3] are thus little known among scientists themselves, although researchers in many fields pick up their ideas “by osmosis” in their post-graduate training.

Sadly this is not at all true of fluid dynamics, particularly as it applies to the environment in the form of numerical models. Generation after generation of ever more complex models succeed one another with very little actual progress, and no improvement at all in realism or relevance. Instead of the exhaustive testing describe by Popper, modellers seek only a single “validation” of their model in the manner of applied mathematicians.

Without Popperian testing, looking to disprove rather than prove, it is possible for major errors and theoretical misconceptions to be carried forward undetected.

A major error they make is in the impulse response function of carbon dioxide concentration due to carbon dioxide emissions widely used by climate modellers and itself based on a circulation model. The impulse response function estimated statistically from time series of the two variables is quite different from the model-derived version [4]. The statistical approach to fluid dynamics proposed in that paper is developed further and applied to other climate-related time series in this paper. Relationships between observed time series are used to help understand macroscopic relationships holding between the variables while making no assumptions about the underlying physics. Such *ad hoc* “laws” are found to have greater predictive power than circulation models while providing fresh insights into likely physical processes.

A theoretical misconception is the idea that fluids can be adequately described as a “continuum”, an infinitely divisible substance, an idea that evolved from the mediaeval concept of a plenum, a space completely filled with matter. “Continuum” works well enough for streamline flows but breaks down mathematically for flows that exceed the critical Reynold’s number [5]. It is a deterministic description that cannot accommodate the stochastic phenomena of entropy and turbulence [6]. The plenum has been abandoned by every branch of physics other than fluid dynamics. Numerical circulation models continue to depend heavily on the continuum concept and on the deterministic equations that support it. Sadly, real-world fluid flows are dominated by turbulence but this is ignored or trivialised in circulation models. Turbulence is even evident in experiments as a Quantum Mechanical phenomenon (e.g. Figure 1e of [7]).

Climate science is, or should be, a branch of experimental physics depending on observation rather than theoretical preconceptions. It is primarily concerned with the relationships between time series of measurable physical quantities and their long term behaviour. Here we develop a rigorous and useful statistical calculus of time series and apply it to real world data. We look at how both global and regional surface air temperature time series are related to atmospheric carbon dioxide concentration. We reveal geographic patterns of climate sensitivity which, to date, have eluded climate modellers.

47 2. Estimating Impulse Response and Sensitivity

48 As discussed more fully in [4], in the absence of a moving average component, the regression
49 model which summarises the relationship between two times series x and y is given by

$$Y_m = \alpha_0 x_m + \sum_{n=1}^p \alpha_n \cdot y_{m-n} + \Xi_m, \quad m = 1, \dots, M \quad (2.1)$$

50 where the regression coefficients, α_i , and their confidence limits are estimated using Ordinary
51 Least Squares. It is termed an ARX(p) model for 'autoregressive with exogenous variable'. The
52 sequence of residuals, $\{\xi_m\}$, is given by

$$\xi_m = y_m - \left(\hat{\alpha}_0 x_m + \sum_{n=1}^p \hat{\alpha}_n \cdot y_{m-n} \right), \quad m = 1, \dots, M \quad (2.2)$$

53 where y_m is the sample value or 'realization' of Y_m and $\hat{\alpha}_0$ to $\hat{\alpha}_p$ are the regression coefficients
54 estimated from the data.

55 The order, p , is found by testing the residuals, $\{\xi_m\}$, for self correlation by means of the Ljung-
56 Box test [8]. The Ljung-Box Q statistic and its probability, P , are calculated for each candidate
57 order, p . The estimated order, \hat{p} , is determined as the least number of coefficients for which P is
58 greater than some predetermined confidence level for which it can be assumed the innovation
59 sequence is not self-correlated.

60 Our best estimate of the relationship between the two time series is given by the convolution

$$\hat{\gamma} * y = \hat{\alpha}_0 x \quad (2.3)$$

61 where

$$\hat{\gamma}_0 = 1 \quad (2.4)$$

62 and

$$\hat{\gamma}_n = -\hat{\alpha}_n, \quad n = 1, \dots, \hat{p} \quad (2.5)$$

63 A more useful form of (2.3) is

$$y = \hat{I} * x \quad (2.6)$$

64 where \hat{I} is given by

$$\hat{I} * \hat{\gamma} = \hat{\alpha}_0 \quad (2.7)$$

65 and is termed the impulse response. For display purposes and inter-comparison a normalized
66 impulse response, \mathfrak{S} , may be used where

$$\mathfrak{S} * \gamma = 1 \quad (2.8)$$

67 Like the regression coefficients, I is a property of the system under investigation and \hat{I} is its
68 estimate. Equation (2.6) describes the output of the system, y , in response to any input sequence,
69 x . The sensitivity of the system, S , is defined here as the response at infinity to a unit step function,
70 H_j , so that

$$S = \sum_{k=0}^{\infty} I_k \quad (2.9)$$

71 i.e. it is the sum of the terms of the impulse response. It is a random variable on which confidence
72 limits can be placed. The sum of a convolution is equal to the product of the sums of the
73 convoluting factors. Hence

$$S = \alpha_0 / \sum \gamma_m \quad (2.10)$$

74 from which \hat{S} can be estimated.

3. Software

The regression model (2.1) was solved using the *OLS* method of the *statsmodels* software package [9] to give estimates, $\hat{\alpha}_i$, of the regression parameters, α_i , from which estimates of the other parameters were derived. The *fit* method of *OLS* returns a class instance *results* with properties specifying the parameter estimates and methods which allow confidence limits to be placed, not only on the parameters themselves, but on any algebraic function of them. For example, (2.4), (2.5) and (2.10) were used to define a constraint in the form of a null hypothesis, \mathcal{H} , viz.:

$$\mathcal{H} : \hat{\alpha}_0 + \hat{S} \sum_{n=1}^{\hat{p}} \hat{\alpha}_n = \hat{S} \quad (3.1)$$

From (3.1) a distribution of the probability of estimated sensitivity, \hat{S} , was found using the t-test method of the *results* class where the relevant R-matrix tuple corresponding to (3.1) was specified as

$$R = ([1, \hat{S}, \dots, \hat{S}], \hat{S}) \quad (3.2)$$

In Table 1, the Ljung-Box parameter, Q , and its probability, P , were calculated using the associated class *statsmodels.stats.diagnostic*.

4. Global Temperature vs ln(CO₂)

We estimated the impulse response of the global average temperature anomaly, T , to the logarithm of atmospheric carbon concentration, $\ln(C)$, rather than to the concentration, C , itself [10]. From this we derived an estimate of sensitivity, S , and its confidence limits using (3.1) and (3.2). Note that sensitivity defined here is the response of the endogenous variable to unit step function in the exogenous variable whereas climate sensitivity, S_c , is defined as the response to doubling of CO₂ concentration. Hence

$$S_c = \ln(2)S \quad (4.1)$$

and similarly for its confidence limits.

Global average temperature anomaly data, T , were taken from the [HadCRUT.4.5.0.0](#) data set [11]. Carbon dioxide concentrations, C , were taken from the University of Melbourne Greenhouse Gas Factsheet[12].

The ARX method was applied to annual means of global average temperature, T_i , on the logarithm of atmospheric CO₂ concentration, $\ln(C_i)$, for the interval 1850 CE to 2014 CE. Applying Ljung-Box to the residuals given by (2.2) for ARX(p), p=0, ..., 5) gives the results shown in Table 1. The probability, P , for the ARX(4) run has a value of 0.2534 indicating that the null hypothesis that the residuals are unselfcorrelated cannot be rejected. Thus the simplest regression

Table 1. Ljung-Box parameter, Q , and its probability, P , for five ARX runs of global average temperature vs. the logarithm of CO₂ concentration.

Run	Variables	Q	P
ARX(0)	T_i vs $\ln(C_i)$ only	284.1	0.0000
ARX(1)	T_i vs $\ln(C_i), T_{i-1}$	49.0	0.0084
ARX(2)	T_i vs $\ln(C_i), T_{i-1}, T_{i-2}$	48.2	0.0074
ARX(3)	T_i vs $\ln(C_i), T_{i-1}$ to T_{i-3}	40.4	0.0358
ARX(4)	T_i vs $\ln(C_i), T_{i-1}$ to T_{i-4}	29.3	0.2534
ARX(5)	T_i vs $\ln(C_i), T_{i-1}$ to T_{i-5}	28.6	0.2367

103 relationship between T_i , and $\ln(C_i)$ which unambiguously fits the data is the ARX(4) model, viz.:

$$T_i = \hat{\alpha}_0 \ln(C_i) + \hat{\alpha}_1 T_{i-1} + \hat{\alpha}_2 T_{i-2} + \hat{\alpha}_3 T_{i-3} + \hat{\alpha}_4 T_{i-4}, \quad i = 5, \dots, N \quad (4.2)$$

104 with the regression coefficient estimates $\{1.161, 0.509, -0.063, 0.057, 0.199\}$.

105 This was used in the t-test method of the *results* class to determine probability as a function
106 of estimated sensitivity. From (2.10), (4.2) and (4.1), we estimated global climate sensitivity as,
107 $S_c = 2.7^\circ\text{C}$ with 95 percent confidence limits of 2.3°C and 3.4°C .

108 5. Regional Temperature vs $\ln(\text{CO}_2)$

109 A netCDF dataset of local mean monthly temperatures for the entire globe was downloaded[13].
110 Each temperature value was associated with a 5 degree latitude by 5 degree longitude spherical
111 rectangle, there being 36×72 such rectangles. Time series of annual averages were computed for
112 each rectangle for comparison with the above-described time series of $\ln(C_i)$ using the ARX(p)
113 method. The Ljung-Box P value was found for candidate values of p in the range $0 < p \leq 5$. The
114 smallest value of p for which

$$P > 0.1 \quad (5.1)$$

115 was chosen as the order of the ARX process and (2.10) solved for S .

116 Spherical rectangles were eliminated from further processing when the number of years of
117 good data was less than fifty or when no value of P satisfying (5.1) could be found. In a surprising
118 number of cases p was zero in which case S was simply the first order regression coefficient of
119 temperature on concentration.

120 Local sensitivity estimates are mapped in Figure 1. For ease of display S values were rounded
121 to the nearest integer.

122 6. Discussion

123 Local climate sensitivity has been mapped before by Asanimov [14] using a similar statistical
124 method. Our map of local sensitivities (Fig 1) and its close resemblance to Asanimov's map
125 demonstrate the viability of the present method. Extreme values tend to lie close together: for
126 example the occurrence of zero values in the North Atlantic and the occurrence of larger values
127 over land. If our method were not working and only generating noise, there would not be such
128 good spatial correlation.

129 High values of in Northern Canada and Siberia suggest that, in these locations, CO_2
130 concentration is the predominant factor controlling nocturnal radiative cooling in the absence
131 of clouds. High regional values in central China have been noted by Eagle *et al* [15]. They
132 were derived from paleoclimate data and attributed by them to the fundamental role played
133 by planetary-scale atmospheric dynamics. Low values in the North Atlantic suggest that other
134 factors, such as submarine volcanism, play a role in modulating Sea Surface Temperature so
135 masking radiative effects. Two unusually high maritime values of $S_c = 4^\circ\text{C}$ off the SE corner of
136 Australia near the island of Tasmania could be due to the intermittent incursion of the warm East
137 Australia Current into this region.

138 Figure 1 is only the first, tantalizing glimpse of the possibilities presented by applying rigorous
139 statistical methods to climate. The effect of CO_2 concentration on other types of observations,
140 such as precipitation, wind speed and so on, remain to be explored. The strong spatial gradients
141 in climate sensitivity observed in places such as California, imply that mean temperature *gradients*
142 are also affected by climate change and this too must have meteorological implications.

143 References

- 144 1 Reid JS. The Sideband Instability and the Onset of Wave Breaking. In: Banner ML, Grimshaw
145 RHJ, editors. *Breaking Waves*. Berlin, Heidelberg: Springer Berlin Heidelberg; 1992. p. 155–159.
146 Available from: <https://apps.dtic.mil/dtic/tr/fulltext/u2/a264196.pdf>.

- 147 2 Popper KR. *Conjectures and Refutations*. New York: Basic Books; 1962.
- 148 3 Kuhn TS. *The Structure of Scientific Revolutions*. Enlarged (2nd ed.). University of Chicago
149 Press.; 1962.
- 150 4 Reid JS. The regression of atmospheric concentration on carbon dioxide emissions.
151 *Geophysical Research Letters*. 2022;Under Review.
- 152 5 Dou HS. No Existence and Smoothness of Solution of the Navier-Stokes Equation. *Entropy*.
153 2022;24(3). Available from: <https://www.mdpi.com/1099-4300/24/3/339>.
- 154 6 Reid J. "The Fluid Catastrophe". Newcastle upon Tyne: Cambridge Scholars Publishing; 2019.
- 155 7 Mukherjee B, Shaffer A, Patel PB, Yan Z, Wilson CC, CrAlpel V, et al. Crystallization of bosonic
156 quantum Hall states in a rotating quantum gas. *Nature*. 2022;601:58–62. See also: https://en.wikipedia.org/wiki/Bose%E2%80%93Einstein_condensate.
- 157 8 Ljung GM, Box GEP. On a Measure of a Lack of Fit in Time Series Models. *Biometrika*.
158 1978;65:297–303.
- 160 9 Seabold S, Perktold J. statsmodels: Econometric and statistical modeling with python. In:
161 9th Python in Science Conference; 2010. Available from: [https://www.statsmodels.org/
162 devel/generated/statsmodels.regression.linear_model.OLS.html](https://www.statsmodels.org/devel/generated/statsmodels.regression.linear_model.OLS.html).
- 163 10 Huang Y, Shahabadi MB. Why logarithmic? A note on the dependence of radiative forcing on
164 gas concentration. *J Geophys Res Atmos*. 2014;119:13,683–13,689.
- 165 11 Morice CP, Kennedy JJ, Rayner NA, Jones PD. Quantifying uncertainties in global and regional
166 temperature change using an ensemble of observational estimates: The HadCRUT4 dataset.
167 *Journal of Geophysical Research*. 2012;117:D08101. Available from: [http://data.giss.
168 nasa.gov/gistemp/taledata_v3/GLB.Ts+dSST.txt](http://data.giss.nasa.gov/gistemp/taledata_v3/GLB.Ts+dSST.txt).
- 169 12 Meinshausen M, Vogel E, Nauels A, Lorbacher K. Historical greenhouse gas concentrations
170 for climate modelling (CMIP6). *Geosci Model Dev*. 2017;10:2057–2116. [https://www.
171 climatecollege.unimelb.edu.au/cmip6](https://www.climatecollege.unimelb.edu.au/cmip6).
- 172 13 Morice CP, Kennedy JJ, Rayner NA, Winn JP, Hogan E, Killick RE, et al. An updated
173 assessment of near-surface temperature change from 1850: the HadCRUT5 data set. *Journal
174 of Geophysical Research: Atmospheres*. 2021;126:e2019JD032361. Available from: [https://
175 www.metoffice.gov.uk/hadobs/hadcrut5/data/current/download.html](https://www.metoffice.gov.uk/hadobs/hadcrut5/data/current/download.html).
- 176 14 Asinimov OA. Predicting Patterns of Near-Surface Air Temperature Using Empirical Data.
177 *Climatic Change*. 2001;50:297–315.
- 178 15 Eagle RA, Risi C, Mitchell JL, Eiler JM, Seibt U, Neelin JD, et al. High regional climate
179 sensitivity over continental China constrained by glacial-recent changes in temperature and
180 the hydrological cycle. *Proceedings of the National Academy of Sciences of the United States
181 of America*. 2013;110(22):8813–8818.

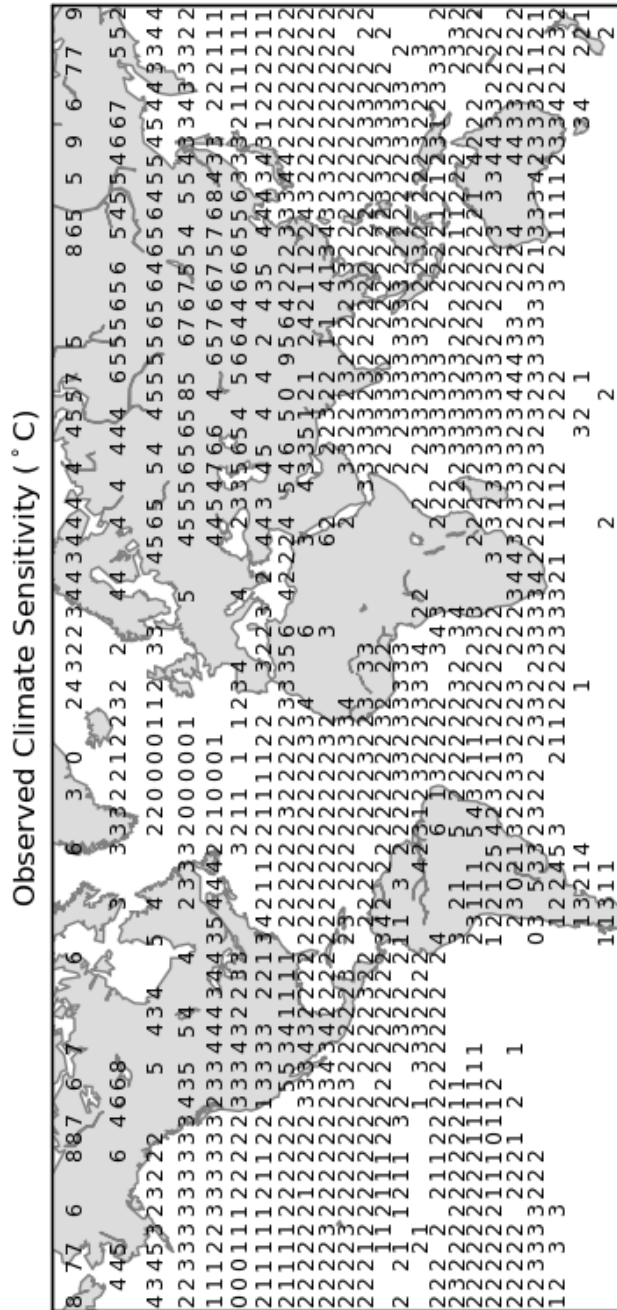


Figure 1. Figure Caption: Climate Sensitivity, S_c estimated for 5 deg X 5 deg rectangles of the earth's surface. Each estimate is derived from the time series of annual average surface air temperature of the rectangle using the ARX method with the time series of $\ln(\text{CO}_2 \text{ concentration})$ as the exogenous variable. Only those estimates from rectangles with more than 50 data points and unselfcorrelated residuals are shown. Displayed values have been rounded to the nearest integer.